

Alfred-Mohammed E, Benson SD, Hirdaris S, Dow RS. [Design safety margin of a 10,000 TEU container ship through ultimate hull girder load combination analysis](#). *Marine Structures* 2016, 46, 78-101.

**Copyright:**

© 2016. This manuscript version is made available under the [CC-BY-NC-ND 4.0 license](#)

**DOI link to article:**

<http://dx.doi.org/10.1016/j.marstruc.2015.12.003>

**Date deposited:**

23/02/2016

**Embargo release date:**

15 January 2017



This work is licensed under a [Creative Commons Attribution-NonCommercial-NoDerivatives 4.0 International licence](#)

# Design Safety Margin of a 10,000 TEU Container Ship through Ultimate Hull Girder Load Combination Analysis

E. Alfred Mohammed<sup>a</sup>, S. D. Benson<sup>a</sup>, S. E. Hirdaris<sup>b</sup>, R. S. Dow<sup>a</sup>

<sup>a</sup>*School of Marine Science and Technology, Newcastle University, UK.*

<sup>b</sup>*Lloyds Register Asia, Technology Group, South Korea.*

---

## Abstract

Assessment of the ultimate longitudinal strength of hull girders under combined waveloads can be of particular importance especially for ships with large deck openings and low torsional rigidity. In such cases the horizontal and torsional moments may approach or exceed the vertical bending moment when a vessel progresses in oblique seas. This paper presents a direct calculation methodology for the evaluation of the ultimate strength of a 10,000 TEU container ship by considering the combined effects of structural non-linearities and steady state wave induced dynamic loads on a mid ship section cargo hold. The design extreme values of principal global wave-induced load components and their combinations in irregular seaways are predicted using a cross-spectral method together with short-term and long-term statistical formulations. Consequently, the margin of safety between the ultimate capacity and the maximum expected moment is established.

*Keywords:* Non-linear FE analysis, Ultimate hull girder strength, Load combination, Container ships

---

## Nomenclature

$\sigma_Y$	Yield strength of the material
$a$	Plate length
$A_B$	Area of the bottom including stiffeners
$A_d$	Cross-sectional area of the deck including stiffeners
$A_s$	Area of one hull side including stiffeners
$B$	Width of inter-frame panel
$b$	Plate breadth
$D$	Depth of the midship section
$F_1$	Longitudinal force
$F_2$	Horizontal shear force
$F_3$	Vertical shear force
$F_4, M_T$	Torsional moment

---

*Email addresses:* emsnoel@gmail.com (E. Alfred Mohammed), simon.benson@newcastle.ac.uk (S. D. Benson), Spyros.Hirdaris@lr.org (S. E. Hirdaris), bob.dow@newcastle.ac.uk (R. S. Dow)

$F_5, M_V$	Vertical bending moment
$F_6$	Horizontal bending moment
$F_h$	Applied horizontal shear force
$F_l$	Applied longitudinal force
$F_v$	Applied vertical shear force
$g$	Distance from the centre of the deck area to the plastic neutral axis
$h_w$	Stiffener height
$M_d$	Design load
$M_h$	Applied horizontal bending moment
$M_p$	Fully plastic moment
$M_t$	Applied torsional moment
$M_v$	Applied vertical bending moment
$M_{TU}$	Ultimate strength in torsion
$M_{VU}$	Ultimate strength in vertical bending
$t$	Plate thickness
$v_s$	Stiffener side deflection
$v_{os}$	Amplitude of stiffener deflection
$w_c$	Column deflection
$w_{oc}$	Maximum amplitude of the column deflection
$w_{opl}$	Amplitude of plate deflection
$w_{pl}$	Plate deflection
$Z_p$	Plastic section modulus

## 1. Introduction

Whereas ship accident statistics show a downward trend [1] advances in reliability based limit state analysis methods for use in ship structural design assessment continue advancing [2, 3, 4, 5]. Innovative research and development aims to ensure asset safety, environmental protection under stringent CAPEX requirements. Limit states directly compare capacity with demand, and are commonly used in combination with partial safety factors which apply to specific scenarios. Ultimate limit state design, which is considered in this study, can enable the use of lower capacity margins to improve economy whilst maintaining an adequate level of safety.

In modern ship structural design the capacity is normally a measure of strength whilst the demand is usually a predicted extreme load case. Perhaps the most essential strength measure for a ship is the ultimate hull girder capacity under longitudinal bending. This measure is traditionally referred to as the ultimate strength of the ship which is a measure of the hull capacity under longitudinal bending conditions [6]. There have been many advances to the ultimate strength problem stemming from the work of Smith [6] and Ueda and Rashed [7], who both developed simplified approaches to predict the progressive collapse of a hull girder under longitudinal bending moment. Advances to these

methods have been proposed to enable general use in longitudinal bending for intact [8, 9, 10] and damaged [11, 12] ships. The Smith method has been incorporated into the latest Harmonised Common Structural Rules for Bulk Carriers and Tankers [13]. Different global load combinations, specifically by incorporating the effects of shear and torsion, have also been considered [14, 15, 16, 17, 18, 19]. For example, the large deck openings and hence low torsional rigidity of modern container ships set this claim against a realistic technical background.

This paper shows how the stochastic combination of torsion with longitudinal bending loads can produce a life-time ship strength safety envelope. The methodology predicts the margin of safety with respect to global loads in two steps. Firstly, the determination of the most extreme global wave-induced load combination that is likely to occur once in the life-time of the structure is evaluated stochastically by a cross-spectral probabilistic analysis method [20]. Secondly, the load carrying capacity of the hull girder is evaluated in conjunction with a combined ultimate strength analysis to establish the margin of safety. The combined ultimate strength calculations are completed using an application of non-linear finite element analysis. Numerical results are presented for the case of a modern 10,000 TEU container ship by interaction diagrams, which conveniently demonstrate the safety margin between the extreme load combinations and ultimate strength under hogging or sagging conditions.

## 2. Background

### 2.1. Longitudinal Strength of a Hull Girder

Over the years, many methods have been employed by classification societies and ship builders for the estimation of the load carrying capacity of the hull girder. Young was the first to calculate the shear force and bending moment distributions along the length of a ship's hull caused by the distribution of the weights of the hull girder and, cargoes as well as distributed buoyancy and wave forces [21].

Attempts to incorporate the effects of plate buckling on ship vertical bending strength assessment were made by Caldwell [22, 23]. He used a simplified procedure where the ultimate moment capacity of a midship cross-section in the vessel sagging condition was calculated by introducing the concept of a structural instability strength reduction factor for the compressed upper longitudinal panels. However, the magnitude of the strength reduction factor was not clearly known at that time [21]. Faulkner [22, 24] further developed this concept by suggesting a design method to calculate this reduction factor. According to Ayyub et al [25, 26], Caldwell's initial approach assumed that the maximum possible ultimate collapse condition is reached when the entire cross-section of the hull, including the side shells reaches the material yield state, under elastic perfectly plastic conditions. This approach suggests that by employing the standard pure plastic bending hinge approach, there is clearly the possibility of plate and longitudinal stiffener buckling of the compressive parts of the structure before the yield limit condition is reached. This simplification means that the fully plastic collapse moment,  $M_p$ , can be expressed as follows:

$$M_p = \sigma_Y Z_p \quad (1)$$

where

$M_p$  = fully plastic moment.

$\sigma_Y$  = yield strength of the material.

$$Z_p = A_d g + 2A_s \left( \frac{D}{2} - g + \frac{g^2}{D} + A_B(D - g) \right) \quad (2)$$

where

$Z_p$  = plastic section modulus.

$A_d$  = cross-sectional area of the deck including stiffeners.

$A_B$  = area of the bottom including stiffeners.

$A_s$  = area of one hull side including stiffeners.

$D$  = depth of the midship section.



$g$  = distance from the centre of the deck area to the plastic neutral axis which is given by

$$g = \frac{D}{4A_s}(A_B + 2A_s - A_d) \quad (3)$$

Similar expressions to equations (1), (2) and (3) have been presented by Kaplan [27] to represent the ultimate bending capacity of a hull girder under two types of failure modes namely: (a) failure resulting from first yielding of hull girder due to pure bending, and (b) failure resulting from full plastic collapse of the entire hull cross-section (including the side shells) [26]. These methods assume that the hull girder is box-like with uniform plate thickness and are generally known as direct methods because of their deterministic nature. They do not consider the influence of initial material and geometric imperfections, which include initial deflections and the residual welding stresses of plating between two longitudinals.

Smith [6, 21, 28], Billingsley [29], Adamchak [30] and Dow et al [22, 31] developed an incremental curvature procedure that allows for the derivation of a moment-curvature relationship for a complete hull. This procedure is commonly known as the Smith's method. This procedure is based on finite element formulations but the plate element strength is obtained from empirical curves. This procedure involves the progressive collapse analysis of a hull girder cross-section under longitudinal bending conditions. The entire hull girder cross-section is divided into small elements made up of plate and stiffener(s) assemblies. The average stress-strain relationships of the individual elements are first derived under the tensile and compressive axial loads considering the influences of yielding and buckling followed by the performance of the progressive collapse analysis. The approach assumes that a plane cross-section remains plane and that each element behaves according to its average stress-strain relationship. This method accounts for the buckling, progressive and interactive behaviour of the failure of structural members, the redistribution of the loads on the hull cross-section after initial buckling and subsequent residual strength of structural members after initial buckling and even after collapse [32]. This contradicts linear elastic theory which assumes that the limiting maximum bending moment sustained by a hull cross-section is equal to the bending moment in way of the first yield.

Other methods include approaches such as the one by Chen et al [33] which was based on a non-linear finite element method. Harada and Shigemi [34, 35] have performed a series of nonlinear finite element analyses for a double hull Very Large Crude Carrier (VLCC) and for a cape size bulk carrier to obtain the ultimate longitudinal strength in hogging and sagging conditions.

A progressive collapse analysis using the Idealised Structural Unit Method (ISUM) which proposed by Ueda [7, 27] has been developed by Paik and Thayamballi [35, 36]. This method evaluates hull girder ultimate strength by considering the effects of initial deflection and the welding residual stresses.

## 2.2. Hull Girder Strength under Combined Loads

The low torsional rigidity of container ships makes them susceptible to developing extensive torsional deformations. In ultimate strength analysis of container ships, it is therefore desirable to study the additional effects of torsion even if those are locally limited to the ultimate strength capacity of the hull girder.

Typical examples of work on this problem include studies by Ostapenko and Vaucher [17] and Ostapenko and Moore [18], who studied the effects of torque in a combined overall loads scenario. More recently, Paik et al [19] studied the ultimate strength of the ship hull under torsion. Their study considers the effects of warping stresses developed under torsion by introducing suitable boundary in way of structural discontinuities (open/closed deck cross-sections). It was concluded that restraining open section warping at the junctions with closed sections, may result in significant stress concentrations. In practice, boundary restraints on a finite element model of a parallel middle body section will induce some stress concentrations. This suggests that a long section, such as a 3-compartment model, should be used to ensure boundary effects are minimised.

In Paik's study, the ultimate strength of ship hulls under a combination of various hull girder sectional load components was calculated numerically either by (a) applying all load components simultaneously and proportionately until the ultimate capacity is reached, or by (b) applying one or multiple load components incrementally until the ultimate limit state capacity is reached, while the rest of the load components are held at a certain constant desired magnitude.

The analyses presented in Paik's paper were undertaken using an adaptation of ISUM.

Based on the calculated results for a typical 4300 TEU container ship, an ultimate strength interaction relationship under combined torsion and vertical bending was obtained via curve fitting as follows:

$$\left(\frac{M_V}{M_{VU}}\right)^{3.7} + \left(\frac{M_T}{M_{TU}}\right)^{3.7} = 1, \quad \text{For hogging,} \quad (4)$$

$$\left(\frac{M_V}{M_{VU}}\right)^{3.1} + \left(\frac{M_T}{M_{TU}}\right)^{3.1} = 1, \quad \text{For sagging}$$

where  $M_V$  and  $M_T$  are vertical bending (hogging or sagging) and torsional moments respectively and  $M_{VU}$  and  $M_{TU}$  are ultimate strength vertical bending (hogging or sagging) and ultimate strength torsional moments respectively. The exponents in Paik's equation can be tuned to adjust the fullness of the interaction ellipse. This may be necessary for different ship types and sizes.

### 3. Methodology for Combined Load Analysis

#### 3.1. Overall Fluid Structure Interaction (FSI) Framework

The analysis completed in this paper is part of a fluid structure interaction approach for evaluating the design capacity margin of an open section hull girder under combined loads. The load prediction is completed using a cross-spectral probabilistic method which is described in [20, 37]. The strength is evaluated deterministically using finite element analysis. A very brief step-by-step summary of the approach is outlined as follows:

1. Determine the Response Amplitude Operators (RAOs) of the ship model;
2. Specify an appropriate Wave Scatter based on operation profile;
3. Carry out cross-spectral probabilistic analysis to predict a desired most extreme global wave load together with other associated global wave loads [20, 37];
4. To determine the structural capacity under combined loads, complete a structural strength analysis of the hull girder under combinations of loads;
5. Determine the design capacity margin by comparing the combined extreme loads determined in 3 with the combined ultimate strength capacity determined in 4.

This paper shows an example application of steps 4 and 5 for a 10,000 TEU container ship. Steps 1-3 have been completed in [20, 37]. In an actual wave loading case in a containership, all extreme global wave loads may be associated with a given principal extreme global wave load. For the sake of brevity, this paper considers a combination of vertical bending moment and torsion moment only with emphasis on methodology. A more detailed study that considers other global wave loads such as horizontal bending moments has been carried out in [37].

#### 3.2. Structural Analysis Method

A NLFEM is used to complete the structural capacity analysis under combined loads. This is compared to the simplified representation of the combined loads using equation (4). Pure vertical bending results

are compared to calculations obtained using the Smith's method. The purpose of the analysis in this paper is to capture the influence of torsion on the longitudinal bending ultimate strength. The dynamic load case that is examined maximises a critical load component and a snap shot of the other load components acting simultaneously. For the case of a containership, because it is an open decks ship, the torsion moment in oblique seas (and hence most of the spectrum) is going to dominate (coupling this with the vertical bending moment also includes the influence in way of beam/following and head seas). Therefore, NLFEM calculations are completed using a two-step quasi-static procedure. Step 1 applies a specific torsion load on the hull girder model. This torsion load is then held constant in step 2 whilst increments of vertical bending moment is applied in order to capture the ultimate strength the bending moment is curvature controlled.

The load is applied in the sequence described under the assumption that longitudinal bending is the dominant component for the determination of the ultimate strength. The torsion, which is applied first, results in shear loading on the plating, predominantly within the closed loop between inner and outer shells. This may result in shear buckling, which has a detrimental effect on the in-plane strength of the plating. The sheared plating is then placed under in plane load from the global bending applied in the second analysis step. In this way the effect of the shear load caused by torsion on the longitudinal ultimate strength is evaluated. In a real scenario the progressive increasing torsion and bending load may occur in phase. This may have some effect on the effectiveness of the plating to withstand in-plane load. However, the exact sequence of loading in a particular event would be highly difficult to predict and therefore the method followed here is judged suitable for the purposes of providing a reasonable measure of the effect of torsion on global bending.

## 4. Structural Modelling and Loading for Nonlinear Finite Element Analysis

### 4.1. Ship Scantlings

A finite element model of the 10,000 TEU OL185 container ship is generated from the details in [Figure 1](#) in conjunction with [Tables 1, 2 and 3](#) where [Figure 1](#) represents the transverse mid ship section of the OL185 container ship which is made-up of the structural elements as defined in [Tables 1, 2 and 3](#). Specifications with respect to the strength of the structural steels used are as follows:

- Scantlings given XH are HT36 steel,  $\sigma_Y = 355 \text{ N/mm}^2$ ;
- Scantlings given XH40 are HT40 steel,  $\sigma_Y = 390 \text{ N/mm}^2$ .

where X represents the letters A, D or E [\[38\]](#). These symbols represent the grading of the higher strength steels that was employed as plating element for most of the upper parts of the longitudinal bulkheads. For example, as can be seen from [Figure 1](#), part of the longitudinal bulkhead distanced 19082mm from the center line (CL) and above deck 2 is made of very thick 73.0 EH steel plating stiffened with mainly  $400 \times 75$  DH flat bars. An elastic perfectly plastic true stress-strain curve is used for both materials.



**Table 1:** Longitudinal bulkheads and side shell longitudinals

Long. No.	L.Bhd. 17310 Off CL	L.Bhd. 19082 Off CL	Side Shell
73		300x75 DH FB	300x75 DH FB
72		400x75 DH FB	400x75 DH FB
71		400x75 DH FB	400x75 DH FB
70		400x75 DH FB	400x75 DH FB
69		400x75 DH FB	400x75 DH FB
68		400x75 DH FB	400x75 DH FB
67		<b>Deck 2</b>	<b>Deck 2</b>
66		320x11/130x15 AH	400x11/150x20 AH
65		320x11/130x15 AH	400x11/150x20 AH
64		<b>Deck 3</b>	<b>Deck 3</b>
63		400x11/150x20 AH	400x11/200x25 AH
62		400x11/150x20 AH	400x11/200x25 AH
61		400x11/150x20 AH	400x11/200x25 AH
60		400x11/200x20 AH	400x11/200x25 AH
59		400x11/200x20 AH	400x11/200x25 AH
58		<b>Deck 5</b>	<b>Deck 5</b>
57		480x11/200x20 AH	440x11/200x25 AH
56		480x11/200x20 AH	440x11/200x25 AH
55		480x11/200x20 AH	440x11/200x25 AH
54		500x11/200x25 AH	500x11/200x30 AH
53		500x11/200x25 AH	500x11/200x30 AH
52	<b>Deck 7</b>		
51	400x11/200x20 AH		
50	400x11/200x20 AH		
49	240x12 AH BP		

**Table 2:** Double bottom girders

Girder	Plating	Stiffener
Girder in center line (CL)	16.5 AH	150x15 AH FB
Girder 3859 off CL	16.5 AH	200x15 AH FB
Girder 6463 off CL	16.5 AH	240x11/150x15 AH
Girder 8953 off CL	16.5 AH	200x15 AH FB
Girder 11443 off CL	16.5 AH	200x15 AH FB
Girder 13933 off CL	16.5 AH	200x15 AH FB
Girder 17310 off CL	16.5 AH	200x15 AH FB

**Table 3:** Other longitudinals

<b>Deck 7 Longitudinals</b>		
Stiffener		Description
No. 22-23		300x11 AH BP
No. 24-25		320x12 AH BP
<b>Inner Bottom Longitudinals</b>		
No. 2-3-4 , 6-7, 10, 12-13, 15-16, 18-19		480x11/200x30 AH
No. 1		480x11/200x15 AH
No. 9		480x11/130x15 AH
No. 20		500x11/200x30 AH
<b>Bottom and Bilge Longitudinals</b>		
No. 1-4, 6-7, 9-10, 12-13, 15-16, 18-19		500x22/200x30 AH
No. 20		500x25/200x30 AH
No. 22, 30-35		370x13 AH BP

#### 4.2. Finite Element Model

The three-compartment model of OL185 container ship modelled in Abaqus CAE is shown in [Figure 2](#). It has two transverse bulkheads separating the compartments and 54 interframe bays with a frame spacing of 791mm.

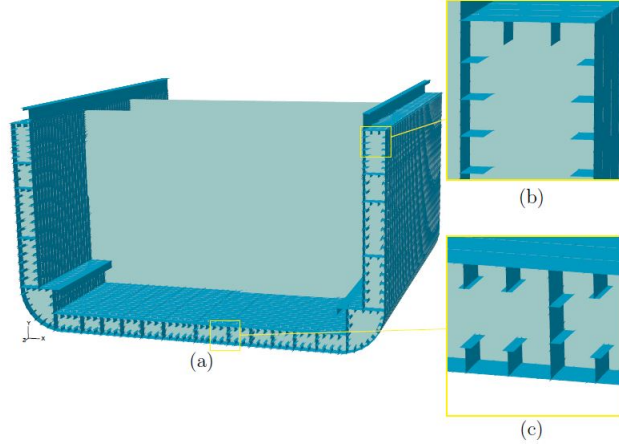


**Figure 2:** (a) A three compartment model of OL185 container ship showing (b) detail section of the upper torsion box region and (c) the bottom plating with the longitudinal stiffening and girders

The meshed model shown in [Figure 3](#) consists of 717,687 linear quadrilateral elements of type S4R and 47,186 compatible linear triangular elements of type S3. S4R is a 4-node doubly curved general purpose shell element capable of reduced integration which makes it computationally less expensive while S3 is a 3-node triangular general purpose shell element [39]. The meshed model is predominated by the S4R elements as the S3 type elements are used in regions with complex geometries including corners and regions of transition between two mesh sizes.

Apart from the shell element selection for the model, the mesh sizes were determined on the basis of relevance and/or region. For example, longitudinal structural elements such as longitudinal bulkheads, bottom and side shell plating and longitudinal stiffeners including the bilge which are considered to have greater influence on the longitudinal strength characteristics of the hull girder were assigned a finer mesh size of 200mm. Thus, for example, there are four elements between the bottom and bilge longitudinals. [Table 4](#) shows the general mesh sizes applied to the container ship hull girder FE model shown in [Figure 3](#).

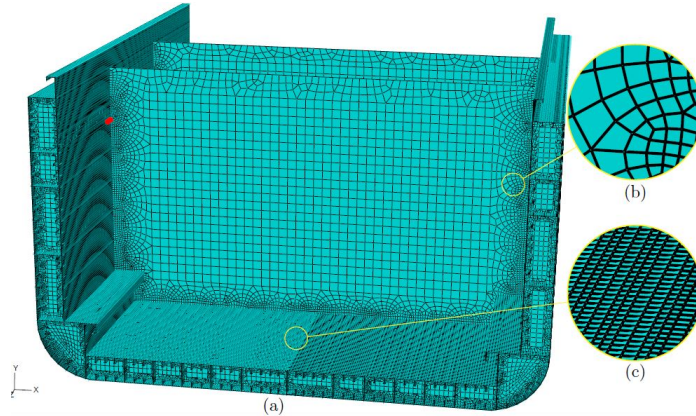


**Figure 3:** (a) The meshed three compartment model of the OL185 container ship showing, (b) the mesh size transition from 800mm to 200mm near the longitudinal bulkheads and (c) the fine mesh size applied to the bottom plating.

**Table 4:** Approximate mesh sizes for OL185 FE model

Structural member	Mesh size (mm)
Longitudinal bulkheads, plates and stiffeners and decks	200
Transverse frames	400
Transverse bulkheads	800

#### 4.3. Initial Geometrical Imperfections

It is well recognised that welding-induced and other initial imperfections significantly affect the ultimate strength characteristics of stiffened plate structures. It is therefore important to model the shape and magnitude of initial geometrical imperfections [40].

There are several different techniques that can be used for imposing imperfections on ship type structures, including [41]:

- imposing deflections on the panel using pressure on one side of the plate;
- superimposing linear buckling mode shapes onto the panel;
- applying displacements to the nodes within a panel based on equations such as defined by Paik et al [40];
- applying displacements to the nodes within a panel based on measured imperfection in experimental as-manufactured panels.

In this study, the direct node translation method employed by Benson [42, 43] was used to superimpose initial geometrical imperfections on the various plate and stiffener components of the OL185 FE model. These superimposed imperfections are standard Fourier series patterns of various mode shapes. Imperfection amplitudes are defined as a function of the nodal positions within the FE model.

The plate imperfection function,  $w_{pl}$ , is defined as [43]

$$w_{pl} = \left( \sum_{i=1}^n \sin \left( \frac{i\pi}{a} u \right) w_{opl,i} \right) \sin \left( \frac{\pi}{b} v \right) \quad (5)$$

where

$w_{pl}$  is the plate deflection;

$w_{opl}$  is the amplitude of plate deflection;

$a$  and  $b$  are the length and breadth of the plate respectively;

and  $t$  is the plate thickness. See Figure 4 for the stiffened panel dimensions.

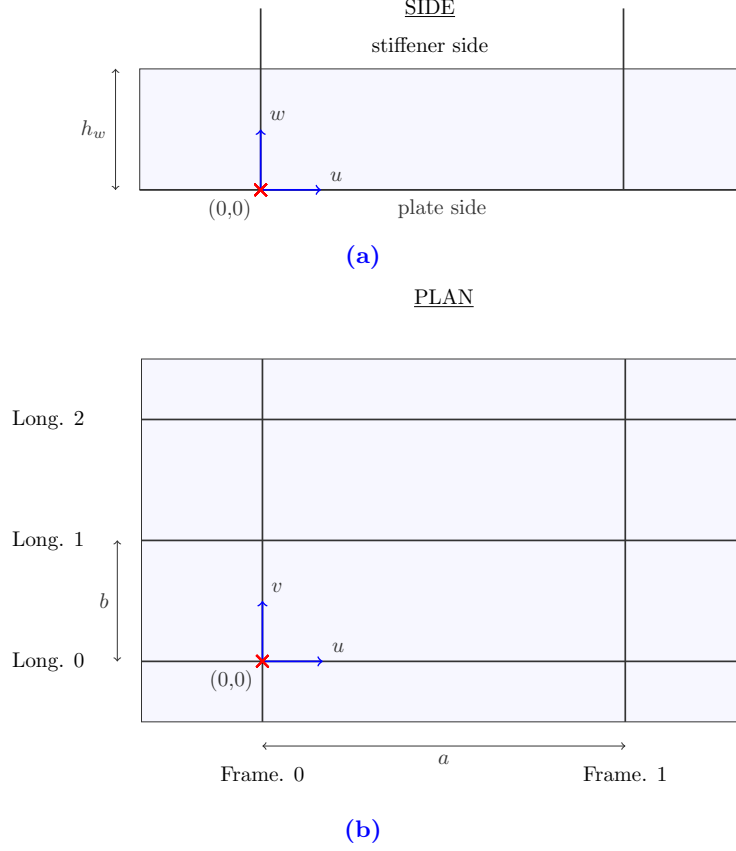


**Figure 4:** Panel coordinate system [43].

The stiffener side deflection,  $v_s$ , depends on the stiffener height and can be expressed by the Fourier series pattern which is given as [43]

$$v_s = F_s \frac{w}{h_w} \sum_{i=1}^n \sin\left(\frac{i\pi}{a}\right) v_{os,i} \quad (6)$$

where

$v_{os}$  is the maximum amplitude of lateral stiffener deflection;

$v_s$  is the stiffener local sideways deflection;

$h_w$  is the stiffener height;

Further overall initial geometric imperfections can be superimposed on whole inter-frame panels in the form of a column deflection,  $w_c$ , applied to all nodes in the panel. This deflection follows a Fourier series sine wave shape with zero amplitude at each frame position. This is given by [43]

$$w_c = \sum_{i=1}^n \sin\left(\frac{i\pi}{B}u\right) w_{oc,i} \quad (7)$$

where

$B$  is the width of the inter-frame panel;

$w_{oc}$  is the maximum amplitude of the column deflection;

$w_c$  is the column deflection.



These formulations have been applied as superimposed deflections in way of the key nodal coordinates of the middle hold of the OL185 container ship (see Figure 5). This ensures the interframe buckling will nucleate away from the model boundaries. Residual stresses are not considered in the analyses due to the large size of the mesh and to ensure convergence of the solution.

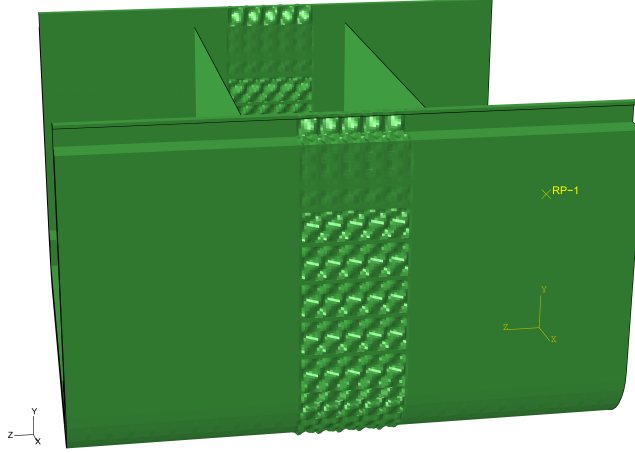


**Figure 5:** An FE model of OL185 showing average imperfection applied at the middle compartment only

#### 4.4. Load Application

For the application of loads, a similar approach to the one adopted by Paik et al [19] is followed. The progressive collapse analysis was completed by fully restraining one end and incrementally applying a load/displacement on a designated reference node RP-1 of the model at the unrestrained end of the FE model. All the nodes in the opposite end have been constrained. A reference node is a node in the model space on which loads (forces, moments or displacements) applied are effectively transferred onto a specific selection of nodes, elements or some other model geometrical entities. Figure 6 shows how sectional forces and moments are applied to the free end of the container ship model at the reference node RP-1.

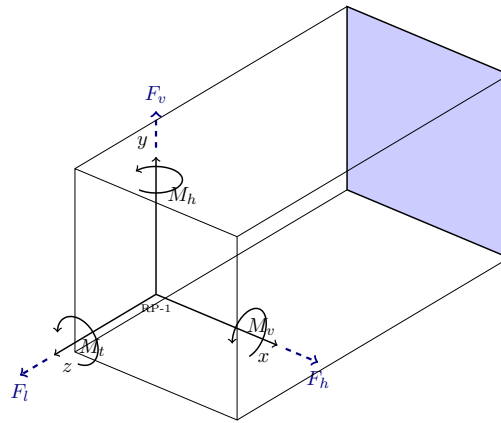


**Figure 6:** Orientation of applied individual sectional shear forces and moments at the reference node RP-1. This illustrates loads application on the FE model where for example,  $M_v$  is applied on the FE model at the reference node RP-1 as an angular displacement (rotation about the x-axis). The coloured end represents the restrained end of the hull girder model.

#### 4.5. Boundary Conditions

All of the node points (highlighted in Figure 7) along the edge of the OL185 FE model have been constrained by applying a fixed boundary condition at the initial step of the analysis. The loads discussed in subsection 4.4 are then progressively applied as boundary conditions in the form of displacements and rotations. The rotations are applied about a single remote reference node, using a rigid body tie constraint to translate displacements to all the edge nodes at the section end whilst keeping the relative position of the nodes to the reference point fixed. This means the end section remains plane. Use of a relatively long three-compartment model ensures boundary effects due to these constraints are minimised. In addition, the rigid body constraint means that the position of the reference point is arbitrary and does not affect the resulting solution.

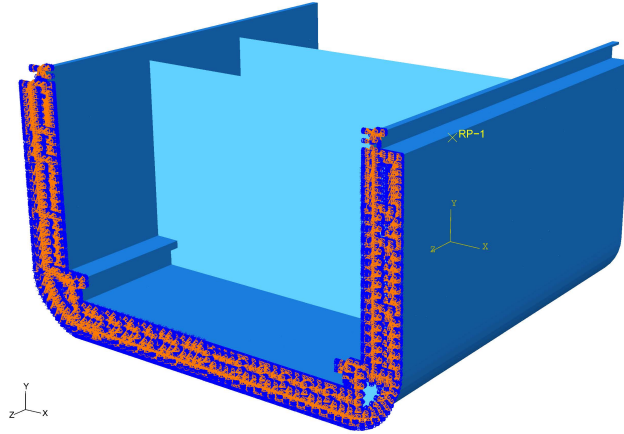


**Figure 7:** FE model of OL185 showing the edge nodes fully constrained against all six degrees of freedom with the applied boundary conditions

### 5. Ultimate Strength in Vertical Bending

To carry out combined strength analysis, it is desirable to ascertain the ultimate strength of the hull girder section in vertical bending alone. To achieve this, a rotation of 0.04 radians was applied incrementally about the  $x$ -axis (see Figure 6) on the reference node RP-1. A rotation of 0.04 radians has been deemed sufficient to take the analysis beyond the ultimate limit state on to the total collapse of the hull girder. This is then repeated for rotations in the opposite direction, thus, creating the effects of both sagging and hogging conditions.

Figure 8 shows the vertical bending moment-curvature relationship obtained from the progressive collapse analysis using two approaches namely the Smith's Simplified Method and the Abaqus non-linear FE code. The following observations can be deduced from Figure 8 for the result from the Abaqus non-linear FE code:

1. The ultimate hull girder vertical bending capacity in the sagging condition is  $2.36 \times 10^{10}$  and in hogging is  $2.345 \times 10^{10}$ ;
2. Similar to the results obtained from the Smith's method, the post-ultimate regime has an almost flattened peak (plateau) however in the Smith's method, the hogging drops off more rapidly. This may be due to the simplifications in the Smith's method for representing hard corners which will be particularly important when the double bottom is placed in compression;
3. The hull girder ultimate strength predicted by the NLFEM shows reasonably good agreement to the simplified method. The bending moment-curvature response also shows good agreement.

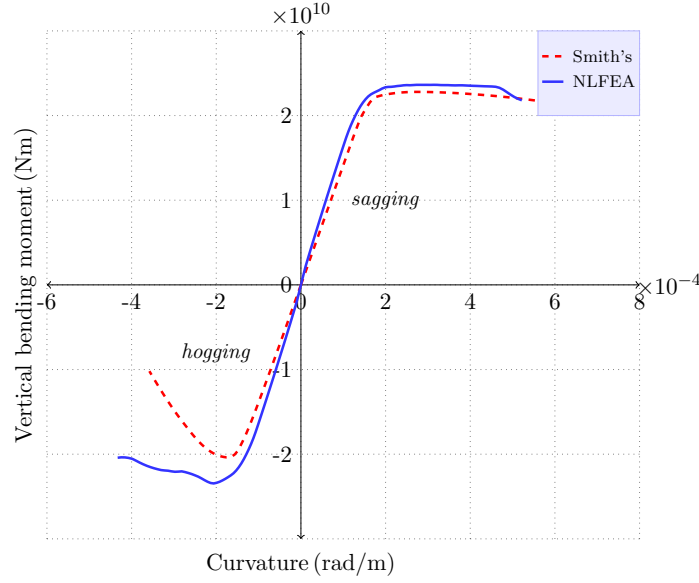
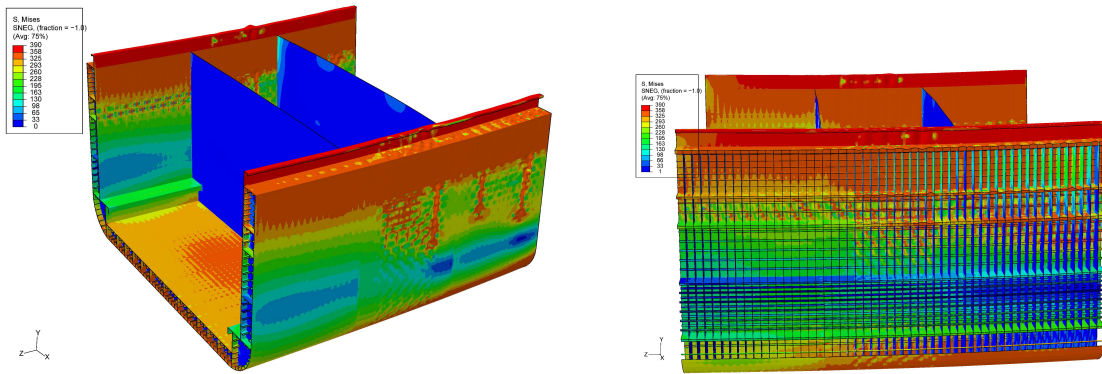


**Figure 8:** Comparisons between the Smith's simplified method and the NLFEA method for the progressive collapse under vertical bending

Figure 9a shows the von Mises stress distribution at the ultimate strength of the hull girder. As expected the instantaneous neutral axis for any section along the length of the hull girder is located closer to the bottom plating. As the vertical bending load is applied incrementally via an applied rotation, the most extreme fibres away from the instantaneous neutral region reach the ultimate compressive/yield strength of the material at the region so that inelasticity/plasticity spreads inwards toward the neutral axis region. This is evident from the pattern of the failed structural members as in Figure 9a where the compression flanges comprising the decks and top side shells and the tension flanges comprising the bottom plating and the bilge are in the plastic regime.



**(a)** von Mises stress distribution on OL185 at the ultimate strength for the sagging moment condition.

**(b)** A view of the longitudinal bulkhead of OL185 showing buckling deformations at the ultimate strength for the sagging moment condition.

**Figure 9:** Views of von Mises stress distribution on OL185 at the ultimate strength under vertical bending moment

Figure 9b shows a view of one of the longitudinal bulkheads. The side shell plating and stiffeners has been removed to show the longitudinal bulkhead from outboards with the vertical stiffened panels, decks

and transverse frames at the ultimate strength of the hull girder under the sagging moment. The hull girder structural collapse proceeds with the failure of the heavy plating and the heavy flat bar stiffeners in the upper deck and the upper region of the bulkhead and the side shell panels. Ultimately, the upper decks and upper side shells fails by buckling at stress levels that are close to the material yield stress of  $390 \text{ Nmm}^2$  as seen particularly in the middle compartment of the FE model in [Figure 9b](#).

## 6. Ultimate Strength in Torsion

The OL185 FE model has two ends; one end is fixed and the other end is unrestrained. The unrestrained end is tied to the reference node RP-1 as a rigid body. Since the end conditions on the model ensures the plane sections at the ends remain plane, warping will be restrained to some degree. The use of a long three-compartment model minimises the effect of this on the resulting ultimate strength solution but does result in some localised stress concentrations close to the model ends, particularly at the model corners.

Torsional moment is applied on the OL185 FE model by applying incremental rotations about the  $z$ -axis (see [Figure 6](#)) until the section is rotated by a value of 0.05 radians at the reference node RP-1. Because the reference node RP-1 is not constrained in the remaining degrees of freedom, it is allowed to warp so that warping stresses are not induced in the hull girder during the non-linear finite element analysis.

[Figure 11](#) shows the von Mises stresses. Note that the torsion box comprising of the upper decks and their corresponding shell plating and stiffeners did not yield and can carry higher torsional loads. This might be responsible for the presence of some positive stiffness in the hull girder between the point where the rotation is 0.01 radians and the ultimate strength as shown in [Figure 10](#) which represents the moment-curvature relationship for progressive collapse of the three-compartment model of OL185 in torsion.

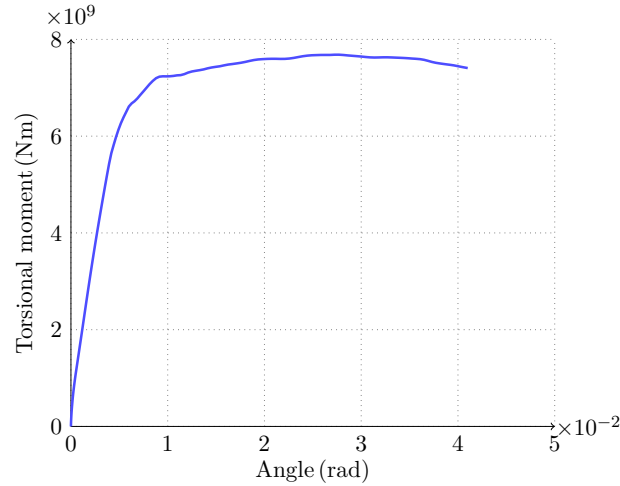


**Figure 10:** A torsion moment-angle relationship for progressive collapse of OL185 under pure torsion

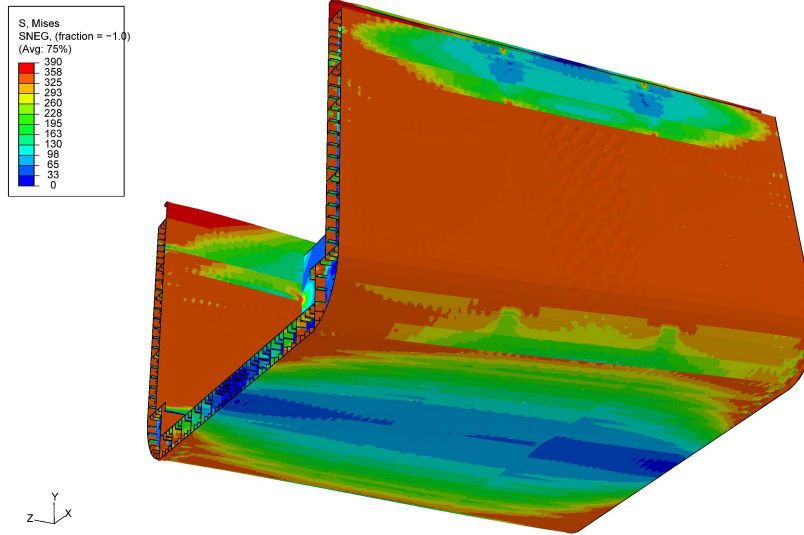


**Figure 11:** von Mises stress distribution on OL185 container ship at its ultimate strength in torsion

## 7. Ultimate Strength under Vertical Bending and Torsional Moments

To further study the load carrying capacity of a hull girder under combined loads, a series of non-linear finite element analyses have been carried out in order to determine the effects of torsional moments on the ultimate strength capacity. The purpose of this is to establish an interaction diagram in which the derived short-term and long-term extreme global wave load combinations that were obtained via a cross-spectral probabilistic methodology [20] can be used to establish the relative margins of the hull girder safety.

### 7.1. Load Application

In this case the moments and rotations were applied in way of the vertical and longitudinal axis of the FE model to model the combined effects of torsion and vertical bending moments respectively. The loads applied at the reference node RP-1 were carried out in steps similar to the methodology introduced by Paik et al [19]. This is described as follows:

- Step 1: The influence of the vertical bending moment is neglected and the torsional moment load is incrementally increased until a desired magnitude is reached at which it is then held (see Figure 6);
- Step 2: The vertical bending moment is then applied in the form of incrementally applied rotations about the x-axis (see Figure 6) until the ultimate strength is reached while continuing to hold the torsional moment at a constant magnitude.

### 7.2. Calculated Results

Eight different magnitudes of torsion were analysed in combination with vertical bending moment as shown in Table 5. Analyses were carried out for both the vertical bending under sagging and hogging conditions. The number of analyses carried out have been considered to be sufficient to describe a representative interaction diagram for the hull girder.

Figure 12 shows the influence of the various magnitudes of applied torsional moment on the ultimate vertical bending strength of the hull girder at the given section. Figure 16 shows the interaction relationship between the vertical bending moment and the torsion for the midship section of OL185 container ship. The vertical bending moment,  $M_V$ , is normalised by the ultimate strength in vertical bending moment alone,  $M_{VU}$ , which is the ultimate vertical bending moment without an applied torsional moment. Similarly, the torsional moment,  $M_T$ , is normalised by the ultimate strength in torsion,  $M_{TU}$ , alone.

**Table 5:** Rotations and torsional moments applied to the reference node RF-1 in the ultimate strength analysis under combined vertical bending moment and torsion

No.	Vertical bend. rotations (rad)	Fixed levels of torsion (Nm) $\times 10^9$
1	0.04	1.00
2	0.04	2.00
3	0.04	3.50
4	0.04	5.00
5	0.04	6.00
6	0.04	7.00
7	0.04	7.50
8	0.04	7.60

From Figure 12, the following conclusions can be made:

- The absolute value of the ultimate strength capacity in both cases of vertical bending moments under sagging and hogging conditions with applied torsion decreases as the torsion is increased. This shows the influence of torsion on the ultimate strength capacity of a hull girder;
- The interaction relationship in Figure 16 shows an interesting relationship between the combined vertical bending moments (in sagging and hogging conditions) and torsion whereby an increase in torsion does not result in a very significant decrease in the longitudinal strength of the hull girder. This is evident even at high levels of torsional load. This behaviour might be attributed to the stockiness of the plates and stiffeners in the torsion box of the hull girder (see Figure 1).

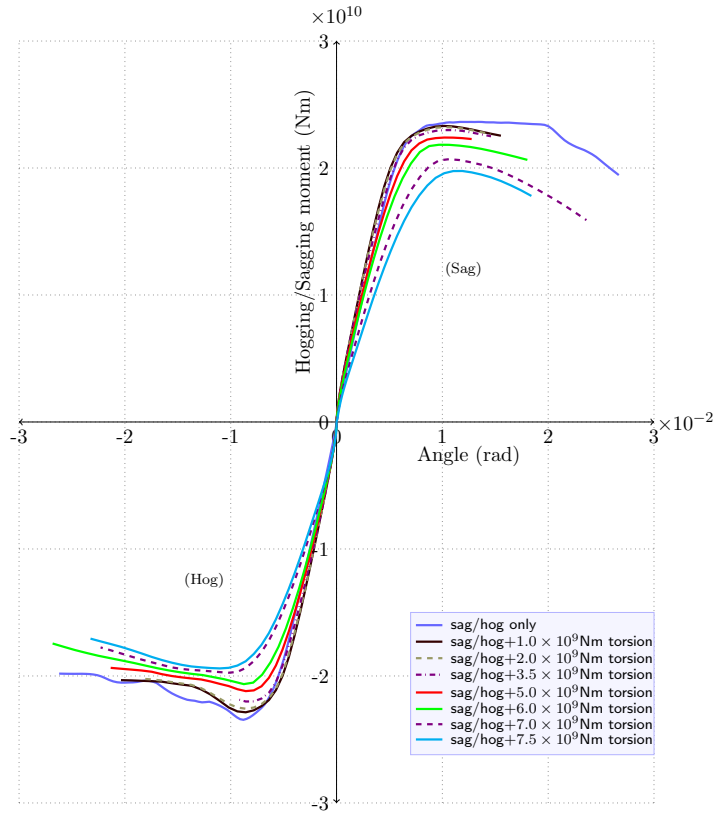
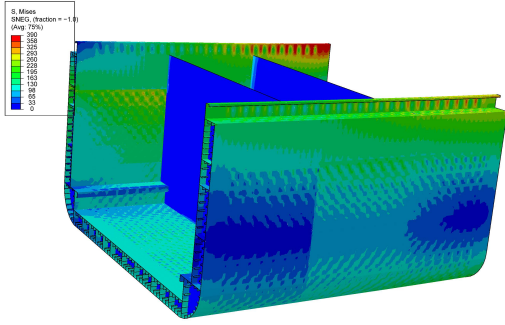
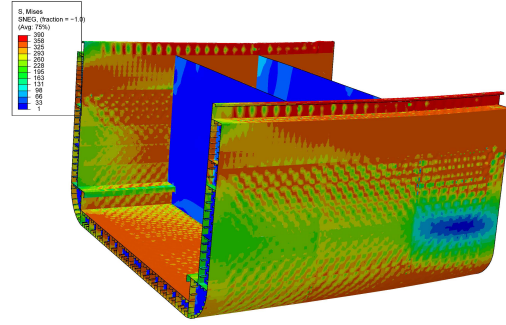


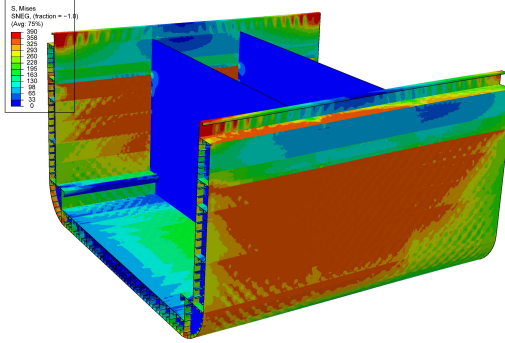
**Figure 12:** Moment-curvature relationships for sagging/hogging moment with torsion for the midship section of OL185 container ship



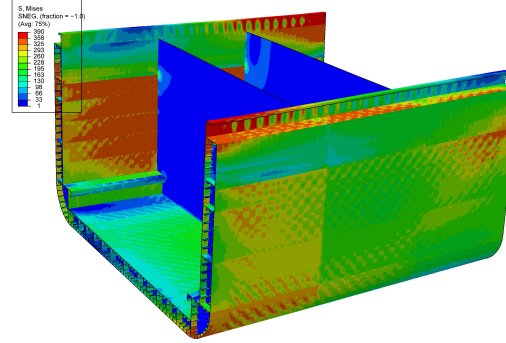
(a) Pre-ultimate strength for combined sagging moment and  $1 \times 10^9 \text{ Nm}$  torsion.



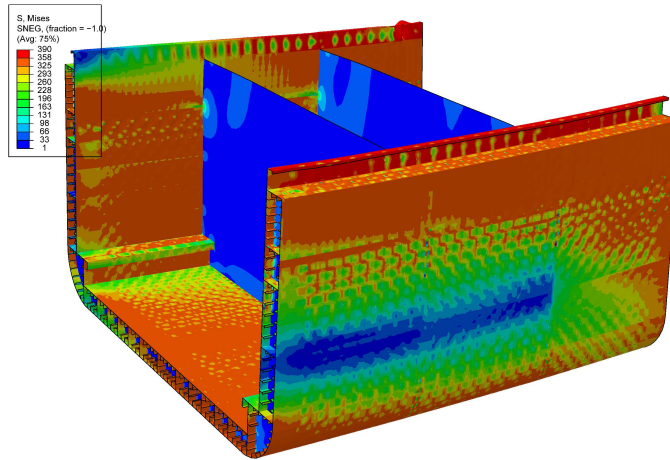
(b) Ultimate strength state for combined sagging moment and  $1 \times 10^9 \text{ Nm}$  torsion.



(c) Pre-ultimate strength with  $5 \times 10^9 \text{ Nm}$  torsion only.



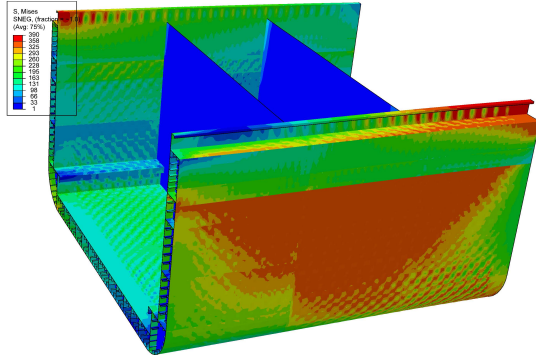
(d) Pre-ultimate strength for combined sagging moment and  $5 \times 10^9 \text{ Nm}$  torsion.



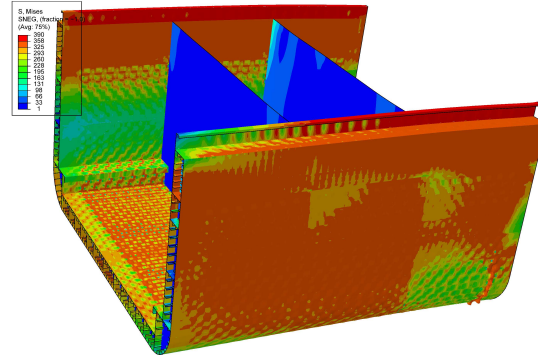
(e) Ultimate strength state for combined sagging moment and  $5 \times 10^9 \text{ Nm}$  torsion.

**Figure 13:** Some cases of von Mises stress distribution on OL185 container ship for combined sagging moments and torsion.

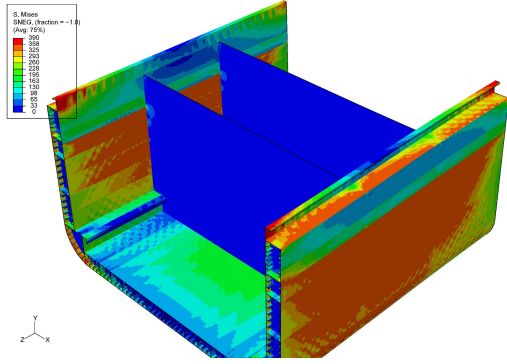




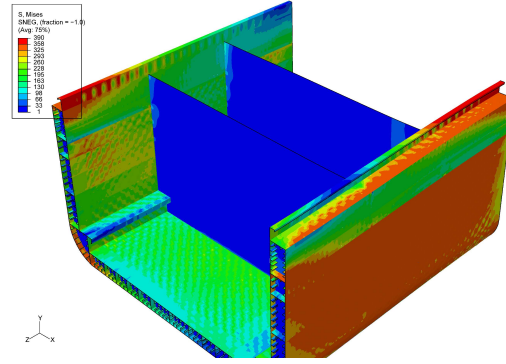
(a) Pre-ultimate strength for combined hogging moment and  $3.5 \times 10^9 \text{ Nm}$  torsion.



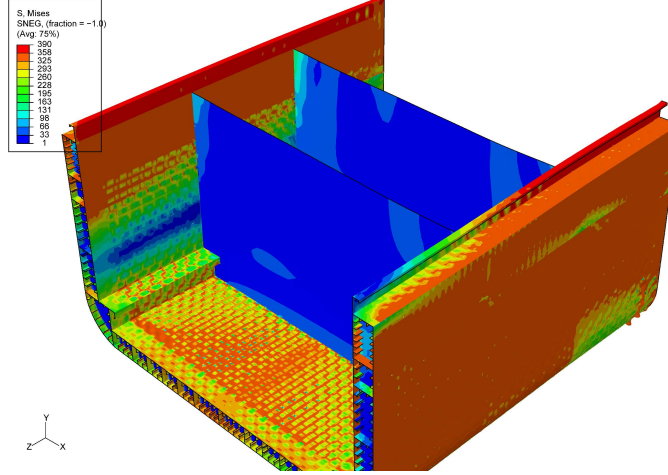
(b) Ultimate strength state for combined hogging moment and  $3.5 \times 10^9 \text{ Nm}$  torsion.



(c) Pre-ultimate strength with  $5 \times 10^9 \text{ Nm}$  torsion only.



(d) Pre-ultimate strength for combined hogging moment and  $5 \times 10^9 \text{ Nm}$  torsion.



(e) Ultimate strength state for combined hogging moment and  $5 \times 10^9 \text{ Nm}$  torsion.

**Figure 14:** Some cases of von Mises stress distribution on OL185 container ship for combined hogging moments and torsion.

Figures 13 and 14 represent snapshots of the highlights of the ultimate strength analyses for combined vertical bending moments (for the sagging and hogging conditions respectively) and the torsional moment.

In these figures, the influence of torsion on the ultimate strength of the hull girder can be seen. For example, let us consider all the results from the the combination of the vertical bending moment in the

sagging condition and torsion.

Figure 13a represents a von Mises stress distribution at a point in the non-linear finite element analysis where the maximum torsion of  $1 \times 10^9 \text{Nm}$  has been applied together with a sagging moment that is close to the ultimate strength. At this point, most of the structural components of the hull girder have not yielded. This behaviour corresponds with the linear section of the corresponding moment-curvature curve in Figure 12. Figure 13b shows a von Mises stress distribution which is similar to the von Mises stress distribution for the ultimate strength of the hull girder under the action of a sagging moment alone as shown in Figure 9a.

Figures 13c show states in the non-linear finite element analyses where the maximum torsion of  $5 \times 10^9 \text{Nm}$  alone begins to cause yielding in the structural members of the hull girder. This is so because this value of torsion is close to the ultimate strength of the hull girder in torsion alone which is  $7.684 \times 10^9 \text{Nm}$  as shown in Figure 10. This explains why the corresponding moment-curvature curve in Figure 12 shows a dominantly non-linear behaviour. Figures 13e shows the von Mises stress distribution at the ultimate strength of the hull girder under combined sagging moment and the respective torsional moments.

The above behaviour for the sagging condition can also be used to explain Figures 14a to 14e which represent snapshots of the highlights of the ultimate strength non-linear analyses for combined hogging moments and torsion.

### 7.3. Extreme Combined Vertical Bending and Torsional Moments

In a reliability based design process, it may be required to compare the most extreme through-lifetime global wave-induced vertical bending moment and the associated extreme torsional moment as obtained through the cross-spectral probabilistic method presented by Alfred et al [20] with the calculated hull girder ultimate strength under the vertical bending and torsional moments for the same hull girder section. For the purpose of this comparison, the load combination from the global wave load combination matrices for both the short-term and long-term load combinations in [20] where the global wave-induced vertical bending moment is the principal load is presented in Table 6.  $F_1, F_2, F_3, F_4, F_5$  and  $F_6$  represent the longitudinal force, horizontal shear force, vertical shear force, torsional moment, vertical bending moment and horizontal bending moment respectively. The long-term combination in Alfred et al [20] is chosen for the ensuing analysis because it features the greater most extreme global wave-induced vertical bending moment.

**Table 6:** Global wave loads combinations at 160.742m from the A.P. for short-term and long-term analyses using the cross-spectral probabilistic method at the most extreme design vertical bending moment

	$F_1$ (N)	$F_2$ (N)	$F_3$ (N)	$F_4$ (Nm)	$F_5$ (Nm)	$F_6$ (Nm)
$C_5$ (short-term)	$4.800 \times 10^7$	$3.278 \times 10^7$	$6.805 \times 10^7$	$2.769 \times 10^8$	$1.174 \times 10^{10}$	$4.407 \times 10^9$
$C_5$ (long-term)	$5.231 \times 10^7$	$3.292 \times 10^7$	$6.794 \times 10^7$	$2.901 \times 10^8$	$1.366 \times 10^{10}$	$4.193 \times 10^9$

The most extreme global wave-induced vertical bending moment with the associated extreme global wave-induced torsional moment from Table 6 is plotted on a modified interaction curve for the ultimate strength analyses for combined vertical bending and torsional moments as shown in Figure 16 in which the shaded region represents a post-elastic region beyond which structural failure occurs.

The plotted point  $P$  which represents the normalised values of  $1.366 \times 10^{10} \text{Nm}$  for the most extreme global wave-induced vertical bending moment and  $2.901 \times 10^8 \text{Nm}$  for the associated extreme global wave-induced torsional moment (see Figure 16) indicates that the extreme global wave-induced vertical bending moment and the associated global wave-induced torsional moment are well within the elastic region therefore the midship section for OL185 container ship is safe against a combination of these extreme loads alone.

A von Mises stress distribution on the midship section of OL185 container ship due to the effect of a load combination comprising of the most extreme global wave-induced vertical bending moment and the associated extreme wave-induced torsional moment is presented in Figure 15. It can be seen that the stress range for most parts of the structure is in the elastic region with the exception of few localised plastic deformations particularly at the hatch coamings and the upper deck.

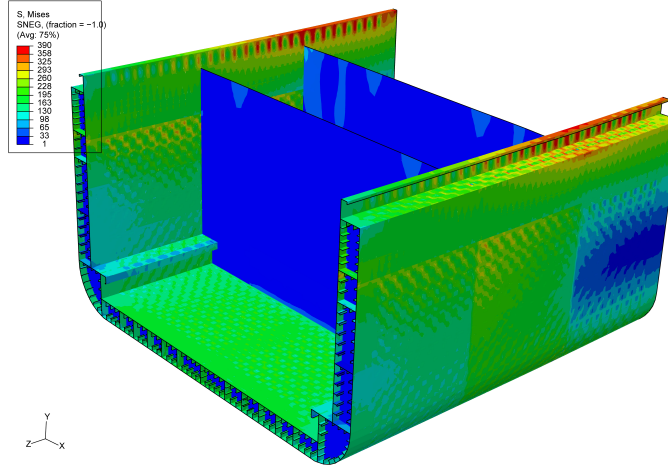


**Figure 15:** von Mises stress distribution on OL185 container ship midship section due the action of the most extreme global wave-induced vertical bending moment and the associated extreme wave-induced torsional moment.

## 8. Hull Girder Safety Margin

The ultimate strength capacity of a hull girder is the maximum load it can sustain and this is usually measured in the midship region of the hull girder. However, prediction of this load without knowledge of the most extreme load that the structure is most likely to encounter once in its life-time is not possible.

Estimation of the design capacity margin therefore requires comparison of the overall bending moment capacities with the design load values. In this sense it is a measure of ultimate limit state (ULS) safety (strength) level built into the hull girder [44].

The ultimate strength capacity  $M_U$  for the OL185 container ship was determined under vertical bending moment and under torsion alone and for load combination types such as vertical bending moment with torsion.

The design loads  $M_d$  here refer to the most extreme loads/load combinations that can be applied for hull girder structural assessment. Global wave-induced loads are implied in this study and their combination consists of the principal most extreme design global wave-induced load and one or more loads that are associated with the principal load (See [20] and subsection 7.3).

The level of safety in the design of the OL185 container ship can be represented by its hull girder design capacity margin  $S$  as [44]:

$$S = \frac{M_U}{M_d} \quad (8)$$

where  $M_U$  is the ultimate strength of the hull girder under a given load type and  $M_d$  is the design load.

Figure 16 shows the load interactions between vertical bending moment and torsional moment by curves which represent the elastic and ultimate limit states. More specifically, Figure 16 shows a load interaction curve between the vertical bending moment and the torsional moment. The interaction ellipse proposed

by Paik in equation (4) is also plotted for reference. Point  $P$  represents a global wave-induced vertical bending moment with its associated torsional moment that has been obtained from a cross-spectral probabilistic load combination analysis in which the global wave-induced vertical bending moment is the principal load [20]. In Figure 16, point  $P'$  represents a combination of global wave-induced vertical bending moment and a corresponding still water bending moment (SWBM) both in the hogging condition for the given frame section together with the associated torsional moment.

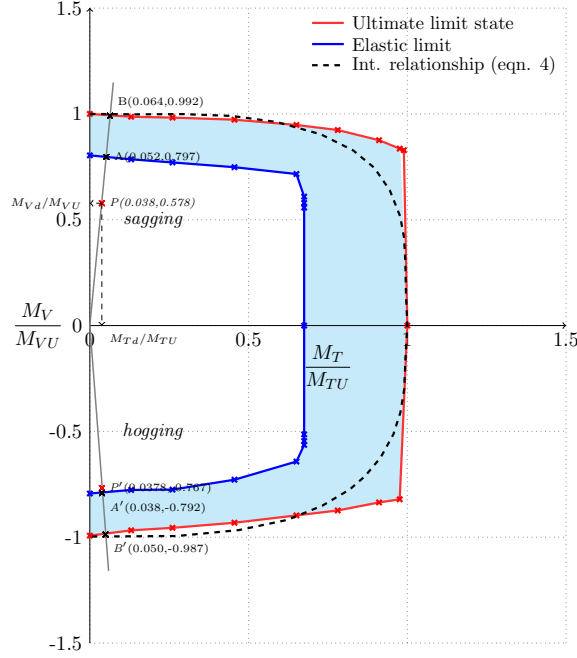


**Figure 16:** Interaction curves showing load combination margins.

The hull girder capacity margin for each load type acting alone is obtained by applying equation (8). For the case of a combined load in which the effect of each load type is taken into account, a line is drawn from the origin of the plots through point  $P'$  and extended beyond the boundaries of the ultimate limit state. Thus, the hull girder design capacity margin with respect to the ultimate limit state (point  $B'$ ) is obtained as:

$$S = \frac{\overrightarrow{OB'}}{\overrightarrow{OP'}} \quad (9)$$

The determination of a hull girder design capacity margin using equation (9) implies a constant load combination factor for a given pair of load types.

Using equations (8) and (9), the various hull girder design capacity margins for single and combined loads have been determined and the results are presented in Table 7 where  $A$  and  $B$  refer to the limit of linearity and ultimate limit state respectively.

**Table 7:** Hull girder design capacity margins

Load Conditions	Load margin wrt A	Load margin wrt B
$M_v$ (sag) only	-	1.74
$M_v$ (hog) only	-	1.72
$M_v$ (sag) + $M_t$	1.38	1.72
$M_v$ (hog) + SWBM	-	1.29
$M_v$ (hog) + $M_t$ + SWBM	1.03	1.28

Comparison between the design load capacity margin for the case of the global wave-induced vertical bending moment under sagging and that for the global wave-induced vertical bending moment (under sagging condition) and its associated torsional moment show that torsion has no significant effect on the hull girder design load capacity margin (see Table 7). This implies that the design of the hull girder of the OL185 container ship is sufficient to sustain the most extreme load combinations involving torsion.

## 9. Conclusions

The combination of wave induced longitudinal bending and torsion loads is especially important to consider for ships with low torsional rigidity such as open deck container ships. This study demonstrates how a probabilistic prediction of combined maximum expected lifetime loads including vertical bending and torsion can be incorporated into the ultimate strength check required in a ship structural design process. This approach enables a direct measure of the design capacity margin compared to the hull girder ultimate strength. This adds a further contribution to interpret strength envelopes as proposed by previous studies such as [17, 18, 19].

The approach is demonstrated using a case study 10,000 TEU container ship. A hull girder ultimate strength envelope incorporating bending moment and torsion was first developed using an application of the nonlinear finite element method. This requires an accurate representation of the geometric and material nonlinear parameters, such as the geometric imperfections in the hull plating, which can significantly affect the calculated ultimate strength. Residual stresses were not included in the model due to the large size of the mesh and to ensure convergence of the solution. To create a strength envelope the finite element model was analysed under pure bending moment, pure torsion, and combinations of both load components. The load is applied in a sequence with torsion applied first and then bending moment applied incrementally up to and beyond collapse. This load sequence is considered appropriate to determine a reasonable strength envelope which demonstrates the interaction of load components. A useful extension to this work would investigate the effect of different load sequences on the strength envelope. Using the bending moment-curvature plots output from the NLFEM both an ultimate strength envelope and an elastic limit envelope were developed. A direct comparison of these envelopes to the results from a cross-spectral probabilistic load analysis may then be completed.

The results show that the vertical bending moment capacity of the hull girder is reduced when torsion is incorporated. The strength reduction for this case study is relatively small under lower levels of torsion but becomes more significant when the torsional component approaches the pure torsional ultimate strength. The probabilistic load assessment shows that the maximum lifetime torsional load component is relatively low compared to the ultimate torsional load ( $M_T/M_{TU} = 0.038$ ) and therefore the ultimate strength assessment is still dominated by longitudinal bending. The design capacity margin is reasonable for both hog and sag load conditions when compared to the ultimate strength envelope, although under hogging conditions the margin to the elastic limit is very small. The margins found in this study are comparable to those found in [45] for a 9,000 TEU container ship with similar structural arrangement.

This study demonstrates that once the strength envelope is defined, the use of a probabilistic load assessment including torsion could be a valuable part of an ultimate strength analysis. It may be that different hull girder cross sections produce different relationships between the bending moment and torsion. Furthermore, this study has assumed a situation where vertical bending is dominant, and has not considered the additional influence of a horizontal bending component. At this point in time, it cannot be concluded if the strength envelope presented here is similar for other ship types or even for other container ships. It can be anticipated that the gradient of the strength envelope as the torsional load component is increased will be some function of the torsional rigidity of the hull. However, significantly more research and validation is required to give a better understanding of this inter-relation. In particular, the influence of asymmetric bending at large angles of heel could be investigated to add a 3rd dimension to the strength envelope. This would add an important extension of this work because it would capture the interaction of all major load components in a real situation. However, the load sequence would need to be considered very carefully.

Furthermore, producing the strength envelope using nonlinear finite element analysis is highly expensive, firstly because of the computational time requirements but also because of the modelling time and expertise required to properly develop the nonlinear mesh model. At present the NLFEM completed in this study cannot be envisaged as part of a normal ship design process. Therefore, the continued development and use of improved analytical methods which can account for different load combinations is still essential. Incorporating torsion into a Smith type analysis method would give the approach presented in this paper much more scope for application in design - not only for the ultimate strength assessment but also for use in scantling optimisation and structural reliability estimates.

## 10. Acknowledgements

The views expressed in this paper do not necessarily express separately or collectively the opinion of Lloyds Register Group Ltd. Dr. Alfred would like to express his thanks to Lloyd's Register Group Ltd. for funding this work as part of his PhD studies at the department of Marine Technology at Newcastle University, UK.

## 11. References

- [1] Germanischer Lloyd. *Best practice in quality and safety management study*. 2013. URL: <http://www.gl-maritime-software.com/news-events/pdf/Best-practice-Studie.pdf>.
- [2] K. Stambaugh, I. Drummen, C. Cleary, R. Sheinberg, and M. L. Kaminski. "Structural Fatigue Life Assessment and Sustainment Implications for a new class of US Coast Guard Cutters". In: *Ship Structure Committee Ship Structures Symposium held in Linthicum Heights, Maryland*. 2014.
- [3] B. M. Ayyub, I. I. Assakkaf, and K. Atua. "Reliability-Based Load and Resistance Factor Design (LRFD) of Hull Girders for Surface Ships". In: *Naval engineers journal* 112.4 (2000), pp. 279–296.
- [4] B. M. Ayyub, I. I. Assakkaf, K. Atua, A. Engle, P. Hess III, Z. Karaszewski, D. Kihl, W. Melton, R. A. Sielski, M. Sieve, J. Waldman, and G. J. White. *Reliability-based Design of Ship Structures: Current Practice and Emerging Technologies*. Society of Naval Architects and Marine Engineers, 2001.
- [5] S. E. Hirdaris, W. Bai, D. Dessi, A. Ergin, X. Gu, O. A. Hermundstad, R. Huijsmans, K. Iijima, U. D. Nielsen, J. Parunov, et al. "Loads for use in the design of ships and offshore structures". In: *Ocean engineering* 78 (2014), pp. 131–174.
- [6] C. S. Smith. "Influence of local compressive failure on ultimate longitudinal strength of a ship's hull". In: *Proc. of the PRADS, International Symposium on Practical Design in Shipbuilding*. 1977, p. 72.
- [7] Y. Ueda and S. M. H. Rashed. "The idealized structural unit method and its application to deep girder structures". In: *Computers & structures* 18.2 (1984), pp. 277–293.
- [8] J. K. Paik, B. J. Kim, and J. K. Seo. "Methods for ultimate limit state assessment of ships and ship-shaped offshore structures: Part III hull girders". In: *Ocean Engineering* 35.2 (2008), pp. 281–286.
- [9] J. M. Gordo and S. C. Guedes. "Approximate method to evaluate the hull girder collapse strength". In: *Marine Structures* 9.3 (1996), pp. 449–470.
- [10] Simon Benson, Jonathan Downes, and Robert S Dow. "Compartment level progressive collapse analysis of lightweight ship structures". In: *Marine Structures* 31 (2013), pp. 44–62.
- [11] RS Dow. "Structural redundancy and damage tolerance in relation to ultimate ship hull strength". In: *Advances in Marine Structures* 3 (1997).
- [12] C. Guedes Soares, R. M. Lus, P. Nikolov, J. Downes, M Taczala, M. Modiga, T. Quesnel, C. Toderan, and M. Samuelides. "Benchmark study on the use of simplified structural codes to predict the ultimate strength of a damaged ship hull". In: *International Shipbuilding Progress* 55.1-2 (2008), pp. 87–107.



- [13] IACS. *Common Structural Rules for Bulk Carriers and Oil Tankers*. International Association of Classification Societies, 2014.
- [14] Zhiyong Pei, Chu Gao, Tetsuya Yao, Yoshiteru Tanaka, Satoyuki Tanaka, Shigenobu Okazawa, Kazuhiro Iijima, Masahiko Fujikubo, et al. “Collapse Analysis of Container Ship Model under Combined Bending and Torsion Applying Idealized Structural Unit Method”. In: *The Twenty-first International Offshore and Polar Engineering Conference*. International Society of Offshore and Polar Engineers. 2011.
- [15] T. Yao, E. Imayasu, Y. Maeno, and Y. Fujii. “Influence of warping due to vertical shear force on ultimate hull girder strength”. In: *9th Symp. Pract. Des. Ships Float. Struct.* 2004, pp. 322–328.
- [16] B Liu and C Guedes Soares. “Study on the ultimate torsional strength of ship hulls”. In: *Marit. Eng. Technol.* 1 (2012), p. 309.
- [17] A. Ostapenko and A. Vaucher. *Ultimate strength of ship hull girders under moment, shear and torque*. Tech. rep. 1980.
- [18] A. Ostapenko and T. R. Moore. *Maximum strength of ship hulls subjected to moment, torque and shear*. Tech. rep. Lehigh University, 1982.
- [19] J. K. Paik, A. K. Thayamballi, P. T. Pedersen, and Y. I. Park. “Ultimate strength of ship hulls under torsion”. In: *Ocean engineering* 28.8 (2001), pp. 1097–1133.
- [20] E. Alfred Mohammed, H. S. Chan, and S. E. Hirdaris. “Global wave load combinations by cross-spectral methods”. In: *Marine Structures* 29.1 (2012), pp. 131–151.
- [21] T. Yao. “Hull girder strength”. In: *Marine structures* 16.1 (2003), pp. 1–13.
- [22] J. M. Gordo, S. C. Guedes, and D. Faulkner. “Approximate assessment of the ultimate longitudinal strength of the hull girder”. In: *Journal of Ship Research* 40.1 (1996), pp. 60–69.
- [23] J. B. Caldwell. “Ultimate longitudinal strength”. In: *Trans RINA* 107 (1965), pp. 411–430.
- [24] D. Faulkner. “Compression strength of welded grillages”. In: *Ship Structural Design Concepts* (1975), pp. 633–712.
- [25] B. M Ayyub, I. I. Assakkaf, J. Sikora, K. Atua, W. Melton, P. Hess, and J. Adamchak. “Reliability based load and resistance factor design (LRFD) guidelines for hull girder bending”. In: *Naval engineers journal* 114.2 (2000), pp. 43–68.
- [26] I. A. Assakkaf, B. M. Ayyub, G. F. M. De Souza, and N. J. Mattei. “Strength Models for Developing LRFD Rules for Hull Girders of Ship Structures”. In: *Structural Safety and Reliability, ICOSSAR* (2001).
- [27] P. Kaplan, M. Benatar, J. Bentson, and T. A. Achtarides. *Analysis and Assessment of Major Uncertainties Associated with Ship Hull Ultimate Failure*. Tech. rep. DTIC Document, 1984.
- [28] C. S. Smith and R. S. Dow. *Ultimate Strength of a Ship’s Hull Under Biaxial Bending (U)*. Admiralty Research Establishment (ARE), 1986.
- [29] DW Billingsley. *Hull girder response to extreme bending moments*. Tech. rep. 1980.
- [30] J. C. Adamchak. “An approximate method for estimating the collapse of a ship’s hull in preliminary design”. In: *Ship Structure Symposium*, ’84. 1900.
- [31] R. S. Dow, R. C. Hugill, J. D. Clark, and C. S. Smith. “Evaluation of ultimate ship hull strength”. In: *Extreme Loads Response Symposium*. Vol. 81. 1981, pp. 133–148.
- [32] Y. Hu, A. Zhang, and J. Sun. “Analysis on the ultimate longitudinal strength of a bulk carrier by using a simplified method”. In: *Marine structures* 14.3 (2001), pp. 311–330.
- [33] Y. Chen, L. M. Kutt, C. M. Piasczyk, and M. P. Bieniek. *Ultimate strength of ship structures*. Society of Naval Architects and Marine Engineers, 1983.
- [34] M. Harada and T. Shigemi. “A method for estimating the uncertainties in ultimate longitudinal strength of cross section of ships hull based on nonlinear FEM”. In: *Proc. PRADS 2007* (2007).
- [35] B. Bhattacharya. “Ultimate Strength Analysis of Ship Hull Girder Under Random Material and Geometric Properties”. In: *Journal of Offshore Mechanics and Arctic Engineering* 133 (2011), pp. 031602–1.

- [36] J. K. Paik and A. K. Thayamballi. *Ultimate limit state design of steel plated structures*. Wiley Chichester,, UK, 2003.
- [37] E. Alfred Mohammed. *Reliability based methodology for the assessment of cumulative life-time hydrodynamic loads and structural capacity*. Marine Science and Technology, Newcastle University, UK, 2014.
- [38] IACS. *Requirement concerning strength of ship - use of steel grades for various hull members for ships of 90m in length and above*. International Association of Classification Societies, 2013.
- [39] Dassault Systmes. *Abaqus 6.10 Online Documentation*. 2010. URL: <http://abaqusdoc.ucalgary.ca/books/usb/default.htm?startat=pt10eli02.html#usb-idx-expelementindex>.
- [40] J. K. Paik and J. K. Seo. “Nonlinear finite element method models for ultimate strength analysis of steel stiffened-plate structures under combined biaxial compression and lateral pressure actionsPart II: Stiffened panels”. In: *Thin-Walled Structures* 47.8-9 (2009), pp. 998–1007. ISSN: 0263-8231. DOI: [10.1016/j.tws.2008.08.006](https://doi.org/10.1016/j.tws.2008.08.006). URL: <http://www.sciencedirect.com/science/article/pii/S026382310800195X>.
- [41] R. M. F. Paulo, F. Teixeira-Dias, and R. A. F. Valente. “Numerical simulation of aluminium stiffened panels subjected to axial compression: Sensitivity analyses to initial geometrical imperfections and material properties”. In: *Thin-Walled Structures* 62 (2013), pp. 65–74.
- [42] S. D. Benson. *Progressive collapse assessment of lightweight ship structures*. Marine Science and Technology, Newcastle University, UK, 2011.
- [43] S. Benson, J. Downes, and R. S. Dow. “A comparison of numerical methods to predict the progressive collapse of lightweight aluminium vessels”. In: *11th International Conference on Fast Sea Transportation FAST*. Vol. 2011. 2011.
- [44] S. Valsgaard, L. Jorgensen, A. A. Boe, and H. Thorkildsen. “Ultimate hull girder strength margins and present class requirements”. In: *Proceedings of the society of naval architects and marine engineers symposium on marine structural inspection, maintenance and monitoring, pp B*. 1991.
- [45] J. K. Paik, G. Wang, B. J. Kim, and A. K. Thayamballi. “Ultimate limit state design of ship hulls”. In: *SNAME Transactions* 110 (2002), pp. 285–308.